Displays 78 (2023) 102451

Contents lists available at ScienceDirect

Displays

journal homepage: www.elsevier.com/locate/displa

# Ultrasonic evaluation of fetal lung development using deep learning with graph

Jiangang Chen [a,b,1], Size Hou [a,c,d,1], Liang Feng [e,1], Bing Lu [f], Minglei Yang [g], Feiyang Sun [c], Qingli Li [a], Tao Tan [h,2,*], Xuedong Deng [f,2,*], Gaofeng Wei [i,2,*]

[a] Shanghai Key Laboratory of Multidimensional Information Processing, East China Normal University, Shanghai 200241, China
[b] Engineering Research Center of Traditional Chinese Medicine Intelligent Rehabilitation, Ministry of Education, Shanghai 201203, China
[c] Department of Applied Mathematics, Xi'an Jiaotong-Liverpool University, School of Mathematics and Physics, Suzhou 215123, China
[d] Department of Mathematical Sciences, University of Liverpool, School of Physical Sciences, Liverpool, United Kingdom
[e] Department of Ultrasound in Medicine, Shanghai Sixth Peaple's Hospital Affiliated to Shanghai Jiaotong Tong University School of Medicine, Shanghai,China
[f] Center for Medical Ultrasound, Nanjing Medical University Affiliated Suzhou Hospital, Suzhou, 215002, China
[g] Artificial Intelligene Innovation Center (AIIC), Midea Group, China
[h] Faculty of Applied Science, Macao Polytechnic University, 5HV2+CP8, R. de Luís Gonzaga Gomes, Macao 999078, China
[i] Naval Medical Department, Naval Medical University, Shanghai, 200433, China

ARTICLE INFO

*Keywords:*
Fetal lung
Fetal cardiac
Image segmentation
Ultrasound image
Graph convolution network
U-net

ABSTRACT

*Background:* The neonatal respiratory morbidity that was primarily caused by the immaturity of the fetal lung is an important clinical issue in close relation to the morbidity and mortality of the fetus. In clinics, the amniocentesis has been used to evaluate the fetal lung maturity, which is time-consuming, costly and invasive. As a non-invasive means, ultrasonography has been explored to quantitatively examine the fetal lung in the past decades. However, existing studies required the contour of the fetal lung which was delineated manually. This may lead to significant inter- and intra-observer variations.

*Methods:* We proposed a deep learning model for automated fetal lung segmentation and measurement, which was constructed combined U-Net with Graph model and pre-trained Vgg-16 network. The graph connection would extract stable feature for final segmentation and pre-trained method could speed up convergence.The model was trained with 3500 datasets augmented from 250 ultrasound images with both the fetal lung and heart delineated manually, and tested on 50 ultrasound images. In addition, the correlation between the size of fetal lung/heart as delineated by the model with gestational age was analyzed.

*Results:* The fetal lung and cardiac area were segmented automatically with the accuracy, average Intersection over Union(IoU), sensitivity and precision being 0.991, 0.818, 0.909 and 0.888, respectively. In addition, the size of fetal lung/heart was well correlated with the gestational age, demonstrating good potentials for assessing the fetal development.

*Conclusions:* This study proposed a new robust method for automatic fetal lung segmentation in ultrasound images using Vgg16-GCN-UNet. Our proposed method could be utilized potentially not only to improve existing research in quantitative analyzing the fetal lung using ultrasound imaging technology, but also to alleviate the labor of the clinicians in routine measurement of the fetal lung/cardiac.

## 1. Introduction

The development of the lung occurs almost last among the organs during the prenatal stage. In actuality, they do not reach complete maturity until the end of pregnancy. By doing a longitudinal study of healthy lung maturation, it is possible to gain a deeper understanding of

* Corresponding authors at: Faculty of Applied Science, Macao Polytechnic University, 5HV2+CP8, R. de Luís Gonzaga Gomes, Macao 999078, China. (T Tan). Center for Medical Ultrasound, Nanjing Medical University Affiliated Suzhou Hospital, Suzhou, 215002, China. (X Deng). Naval Medical Department, Naval Medical University, Shanghai, 200433, China. (G Wei).
*E-mail addresses:* taotanjs@gmail.com (T. Tan), xuedongdeng@163.com (X. Deng), highpeak8848@163.com (G. Wei).
[1] Jiangang Chen, Size Hou and Liang Feng were equally Contributed.
[2] Gaofeng Wei, Xuedong Deng and Tao Tan were equally corresponded.

https://doi.org/10.1016/j.displa.2023.102451
Received 16 January 2023; Received in revised form 21 March 2023; Accepted 24 April 2023
Available online 28 April 2023

the pulmonary anatomy in the premature newborn. [1]Any abnormity associated with the fetal lung development, in particular the lung immaturity, may lead to serious mortality and morbidity, such as respiratory distress syndrome or transient tachypnea of the newborn [2]. According to DeSilva et al. [3], pulmonary surfactant is the primary factor that determines the development of the fetal lungs and could only be measured through laboratory testing on amniotic fluid. Now, the necessity for non-invasive methods to accurately estimate lung maturity has become apparent.. Although the gestational age was commonly used as an important indicator for the lung immaturity, itsuffered from low correlation in between. Alternatively, the size or volume of the fetal lung was measured to assess the fetal lung development using medical imaging technologies, e.g., magnetic resonance imaging(MRI) and ultrasound [4–7]. Therein, ultrasound was considered as a promising means for assessing the lung immaturity due to its economic efficiency and easy operation.

However, precise evaluation of lung maturity using ultrasound highly relied on the experience of the sonographers. To alleviate such a dilemma, various computer-assisted methods were applied to quantitatively analyze fetal lung evaluation. Feingold et al. [8]analyzed the ratio of the ultrasonic reflectivity of the fetal lung to the liver with the aim of quantitatively assess the fetal lung maturity.Mottetet al. [9]evaluated the stiffness of the fetal lung which was correlated with the fetal lung development using shear wave elastography. Tekesin et al. [10] analyzed the histogram of the fetal lung area in the ultrasound images to perform quantitative ultrasonic tissue characterization to evaluate the fetal lung development. Palacio et al. [11] attempted to assess the maturity of the fetal lung by analyzing the texture information of the fetal lung using ultrasound, which was considered changing at different gestational weeks. Such a change could not be interpreted by humans but computers with intelligent algorithms. However, existing methods were dependent of the lung region delineation on human [11–13] which was labor-intensive and error-sensitive. In addition,inter-operator deviation and bias may exacerbate the accuracy of the final evaluation.

To discriminate between the regions of interest and the background organs and tissues that can be disregarded in US images, segmentation techniques could be used. Also, this method can offer imaging biomarkers for forecasting fetal development and prognosis. To evaluate the health of the fetus and forecast problematic pregnancies, it is possible to quantify the shape, volume, morphometry, and texture of the fetal organs while they are developing [14]. New chances to intervene and safeguard at-risk fetuses are created by early biomarkers of prenatal organ illness that may harm fetal growth and wellbeing.

With the low signal-to-noise ratio of US images [15], segmenting the fetal lung has become a challenging undertaking. Fetal chest ultrasound is particularly affected by speckle noise and signal dropout, which causes weak contrast and fuzzy borders (poor image quality) [16]. Because the tissue densities of the fetal lung and heart myocardium are similar [17], segmenting the fetal lung effectively is similarly challenging. In this research, we focused on the intelligent segmentation of fetal lung and heart and evaluation their development.

Recent advance in image segmentation focused on the the application of the deep learning. In this respect,Havaei et al. [17] attempted tosegment the brain tumor in a fully automatic manner using deep neural networks. Hossain et al [18] developed a method with a modified U-Net network for segmenting micro-calcification regions of mammogram images. Hu et al. [19] tried to segment the lung region on Computed Tomography(CT) images using region convolutional neural networks(Mask R-CNN) associated with supervised and unsupervised machine learning. In our previous work, the region of the fetal lung was automatically segmented using U-Net with pre-trained Vgg-16 network.

In the fetal lung segmentation field, Kainz et al. created the first semi-automatic technique for fetal thorax examination [20]. To train a forest ensemble approach for the localization of the spina cord, a fast rotation invariant spherical harmonic descriptor was created. To perform a geodesic active contours segmentation, voxels that were initial foreground/background constraints for each class were created. This method requires too much manual post-processing by experts and cannot form an automatic semantic segmentation model. In Chikop et al.'s rendering of a lung volume to illustrate the biometric measurements necessary to ascertain fetal developmental rates in pathology characterization, an active contour method was also used [21]. After segmentation, morphological methods were used to eliminate erroneous regions. Using the use of Haar wavelet and Fourier transform filtering, the banding artifact was removed. The above method relied on a-priori information of the image based on hyper intensities and were multi-stage models.

A straightforward CNN segmentation model created by Rajchl et al. [22]was influenced by LeNet architecture. They chose a CRF with several connections was one of the post-processing steps. They could not use deep learning models to form an end-to-end segmentation method. In Wang et al. [23] a deep-learning framework was also used to generate a 2D segmentation of the embryonic brain, placenta, and lungs. In a bounding box and a pipeline based on scribbles, authors linked CNNs. Due to a weighted loss and an image-specific fine-tuning, the suggested method outperforms conventional interactive segmentation approaches. The algorithms were common CNN methods, which will face the challenge of poor US image quality.

In this work, we proposed the U-shaped Graph Convolution Network (GCN) with Visual Geometry Group 16 layers module (VGG16), which is a novel segmentation model by segmenting the fetal lung. It consisted of a VGG16 blocks as the encoder, convolution blocks as the decoder, and skip-connections with a GCN as the bridge. In the encoder, we replaced the convolutional module in original UNet with a VGG16 module to enhance the local feature extraction capability while obtaining abstract feature. The bridge with GCN connection optimized the fusion of long-range information and context information between the encoder and the decoder [24]. GCN continuously strengthened the representation of intermediate feature maps to find a low-dimensional invariant topology, improving the extrapolation of segmentation models. GCN bridge will build relationship in pixels of image, which is stable topological feature (structure feature). [25–27]Our model leveraged advantages of both convolutions and graph models, i.e., proper generalization ability and sufficient model capacity [28].

## 2. Materials and methods

### 2.1. Image acquisition and ROI labeling

The data was retrospectively collected from the Department of Medical Ultrasound, Nanjing Medical University Affiliated Suzhou Hospital, Suzhou, China. The ultrasound equipment is WS80A with Elite (Samsung Medison, Seoul, Korea) equipped with a curved array ultrasound probe (CA1-7A). Totally 300 ultrasound images were collected at the four-chamber view in the conditions ofi) the fetal heart at the diastole phase; ii) one half of the fetal lung close to the probe, and iii) the fetal spine at the direction of either 3 or 9o'clock. The data were stored as Digital Imaging and Communications in Medicine (DICOM) format. A sonographer in fetal ultrasound field with over6-year experience delineated the fetal lung and heart regions using Labelme [29], showed in Fig. 1. The annotation of fetal lung and heart region was served as the ground truth for evaluating the performance of the automated segmentation technique subsequently. The input of our model is fetal US image stacked in three channels as shown in Fig. 1 a. The outputs are the segmentation results of Lung and Heart in US image as show in Fig. 1 b. This study was approved by the ethics committee of Nanjing Medical University Affiliated Suzhou Hospital, Suzhou, China, with the written informed consent waived ((Approval number: K2016038).

### 2.2. Image processing and data augmentation

Every image read in the DICOM format was cropped with the field of

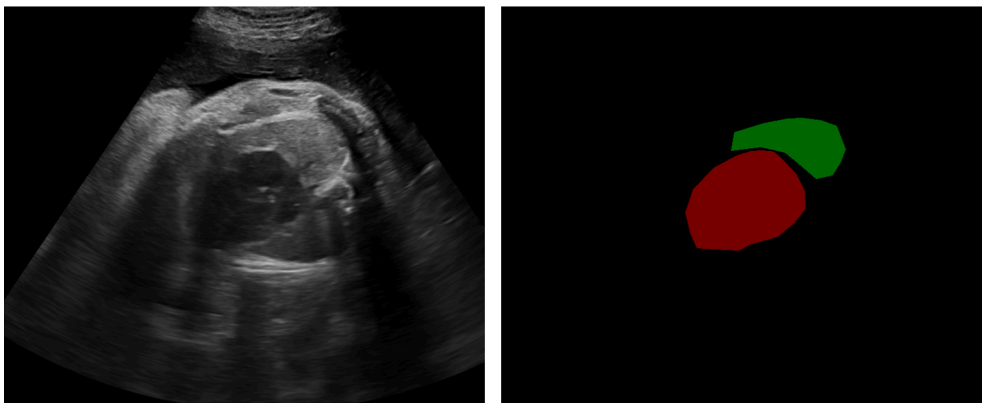


**Fig. 1.** A. fetal ultrasound image at four-chamber view; b. region of labels, green: fetal lung, red:fetal heart. (For interpretation of the references to colour in this figure legend, the reader is referred to the web version of this article.)

ultrasound image remain. One of the three RGB channels was chosen for the following process. Subsequently, data augmentation was applied to the training data set via rotation, flip, and shift transformation which is broadly used in deep learning [30], to increase the quantity of training data and improve the robustness of the model. Such a progress increased the image number from 250 to 3500 (50 original images for test remaining).

### 2.3. UNet model with pre-trained Vgg-16 network

Large medical data are difficult to collect in healthcare. In the study, the proposed model for the semantic segmentation of fetal lung images was based on the U-Net network recognizing its good performance insegmentation of medical images [31].

The full convolutional network (FCN) [32] was the foundation of U-Net. U-Net executed skip connections at the same stage between the encoding and decoding as FCN and had four decoding modules in comparison [33]. As a result, it could be ensured that the final restored feature map may fuse multi-scale features to provide multi-scale prediction and deep supervision in addition to combining high-resolution and high-level semantic information.

Four encoding modules and four decoding modules were applied in this investigation. A max-pooling layer, two 3x3 convolution layers, and an up-sampling operation were included in each encoding module and each decoding module, respectively. As a result, the resolution of the output feature matched that of the input feature. Each convolution layer was followed by a rectified linear unit (ReLU) function and a batch normalization layer [34–35] to ensure convergence [36]. Fig. 2

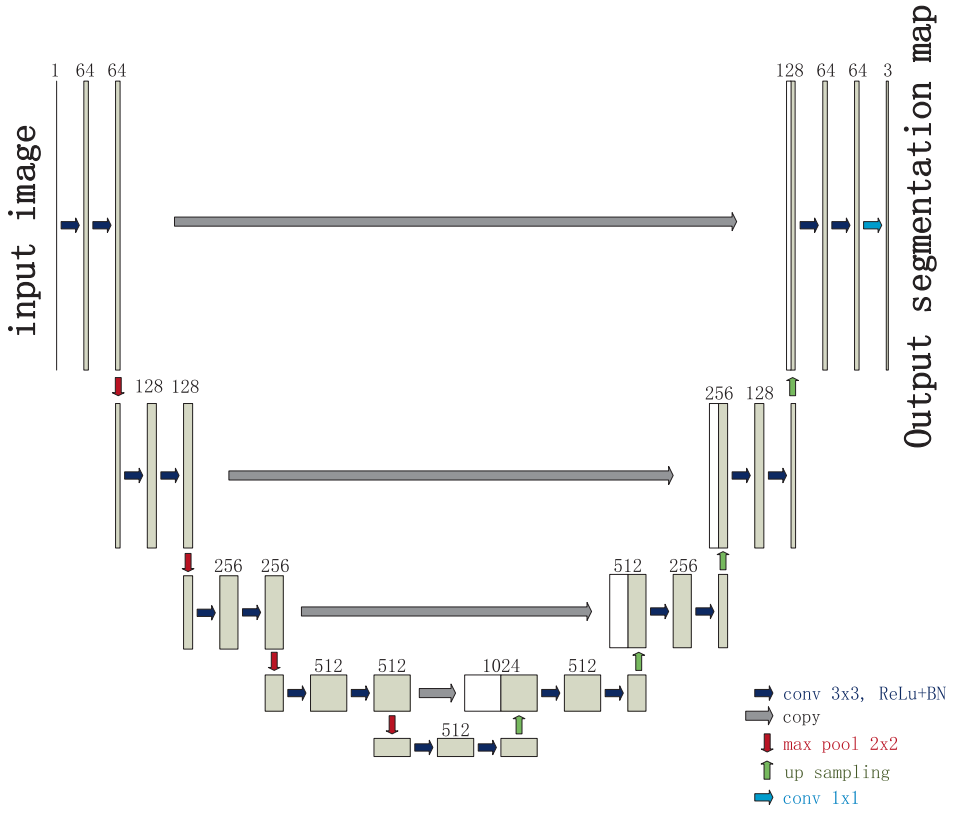


**Fig. 2.** U-net network architecture.

illustrates the design of the U-Net employed in this investigation.

To extract features for large-scale images, VGG-Net used deep convolutional layers [37]. VGG-Net, which is a derivative of Alex-Net [38], employed tiny (3x3) convolutional filters in every layer. One 5x5 convolutional layer and two cascaded 3x3 convolutional layers have the same effective reception field, but the later architecture has less parameters to train [39]. In this study, we merged the U-Net downsampling architecture with the VGG16 network, which had 13 convolutional layers and 3 fully connected layers. Furthermore, in order to speed up the training process and reduce over-fitting, transfer learning [40] was applied in our work.

### 2.4. GCN bridge

We multiplied feature map with its transposed to get node features after encoder. Global relationship node feature will be updated by two layers of GCN blocks. Finally, the final feature map could be fused between origin encoder output and global relationship node feature. The Graph bridge is shown in Fig. 3.

Our model aimed to cluster the hidden feature map's graph which encoded by VGG16-U-Net by GCN. This part would be based on spectral graph convolutional operation, which means to extract the properties of graph by the eigenvalues and eigenvectors of the Laplacian matrix of the graph.

According to the convolution theorem Eq. (1), the graph convolution operation could be changed to find the inner production of two signals' Fourier transformation.

$$F(k(t_1)*k(t_2)) = K_1(w)K_2(w) \tag{1}$$

When the input graph would be decomposed, it will get linearly independent vectors which compose the orthogonal basis of Fourier transformation. The Fourier transform on graph is formulated as:

$$\widehat{k} = U^T k \tag{2}$$

Hence, the GCN block is formulated as:

$$H(L+1) = \sigma\left(D^{-\frac{1}{2}}LD^{-\frac{1}{2}}H(L)W\right) \tag{3}$$

A local feature map *Xr* in the latent space is fed to two convolutional layers in parallel to generate two maps: one feature map with reduced dimension and one projection matrix. After that, the reduced dimension feature is reshaped, while the projection matrix is reshaped and transposed to *Xa*. A matrix multiplication between *Xr* and *Xa* is then performed to obtain a node feature map before its being sent to a GCN block.

GCN models are a special form of Laplace smoothing. It combined the structure of the graph and the features of the vertices in the convolution, and the features of the unlabeled vertices are mixed with the adjacent marked vertices, and then propagated on the network through multiple layers [41]. Laplacian smoothing computed a new feature of a pixel, which was a weighted average of the pixel itself and its neighbors. Because pixels of the same cluster tended to be more closely connected. But if there were more than two GCN layers, it would be difficult to train. And repeated use of Laplacian smoothing may mix the features of vertices in different clusters, making them indistinguishable.

There are two novelties in our proposed model. Firstly, we proposed GCN connection to replace skip connection in bridge of encoder and decoder. GCN bridge could combine the similar feature to build the stable topology feature in segmentation task. Secondly, we used pre-trained VGG model to extract the US images feature. Pre-trained model has been trained in a very large dataset which included natural images, which can discover the high-dimensional features of the data, and the features required by the target task can be extracted from these high-dimensional features. Therefore, freezing the weight of the pre-training layer would reduce the amount of the whole parameters. It can help the model accelerate convergence and overcome the obstacle of over-fitting.

## 3. Results

The performances of all the proposed models were compared, as listed in Table 1 and Table 2. Three segmentationresultsare shown in Fig. 4 and Fig. 5, representatively. Figs. 6 and 7illustrate the Bland-Altman analysis for testing the agreement between the automated and manual segmentations of the fetal lung and heart, respectively. The changes of the sizes of the fetal lung and heart extracted from the segmentation results were plotted in terms of gestational age (31st to 41st week), as shown in Figs. 8 and 9. The size of fetal heart increased gradually with the development of fetus from week 31 to week 41 ($P < 0.0005$). Post-hoc comparisons showed statistical difference between week 31 and weeks 38 to 41 ($P = 0.005$ for week 31 vs week 38, $P = 0.019$ for week 31 vs week 39, $P = 0.001$ for week 31 vs week 40, $P = 0.045$ for week 31 vs week 41) and week 32 and weeks 38 to 41 ($P =$

**Table 1**
Comparative Experiment in Validation set.

| Method | Metric | | | |
|---|---|---|---|---|
| | Accuracy | Recall | Precision | IOU |
| U-Net without cardiac | 0.993 | 0.838 | 0.825 | 0.702 |
| U-Net with cardiac | 0.988 | 0.842 | 0.880 | 0.751 |
| Vgg16-UNet without cardiac | 0.995 | 0.860 | 0.873 | 0.757 |
| Vgg16-UNet with cardiac | 0.990 | 0.883 | 0.882 | 0.786 |
| Attention-U-Net without cardiac | 0.994 | 0.730 | 0.930 | 0.683 |
| Attention U-Net with cardiac | 0.989 | 0.853 | 0.884 | 0.762 |
| GCN U-Netwithout cardiac | 0.994 | 0.860 | 0.839 | 0.736 |
| GCN U-Netwith cardiac | 0.988 | 0.828 | 0.891 | 0.751 |
| VGG16-GCN U-Netwithout cardiac | 0.995 | 0.850 | 0.892 | 0.765 |
| VGG16-GCN U-Netwith cardiac | 0.991 | 0.909 | 0.888 | 0.812 |

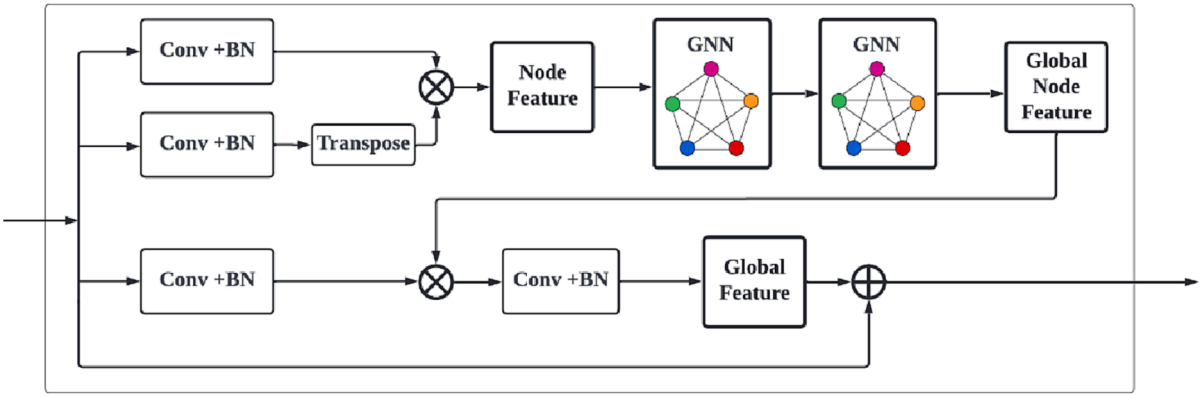


**Fig. 3.** GCN bridge.

**Table 2**
Comparative Experiment in Test set.

| Method | Metric Accuracy | Recall | Precision | IOU |
|---|---|---|---|---|
| U-Net without cardiac | 0.980 | 0.514 | 0.831 | 0.481 |
| U-Net with cardiac | 0.961 | 0.611 | 0.868 | 0.560 |
| Vgg16-UNet without cardiac | 0.983 | 0.622 | 0.833 | 0.582 |
| Vgg16-UNet with cardiac | 0.964 | 0.647 | 0.874 | 0.599 |
| Attention-U-Net without cardiac | 0.977 | 0.367 | 0.856 | 0.355 |
| Attention U-Net with cardiac | 0.957 | 0.564 | 0.863 | 0.518 |
| GCN U-Netwithout cardiac | 0.981 | 0.598 | 0.830 | 0.555 |
| GCN U-Netwith cardiac | 0.961 | 0.616 | 0.863 | 0.566 |
| VGG16-GCN U-Netwithout cardiac | 0.982 | 0.614 | 0.844 | 0.579 |
| VGG16-GCN U-Netwith cardiac | 0.967 | 0.675 | 0.892 | 0.633 |

0.003 for week 32 vs week 38, P = 0.013 for week 32 vs week 39, P = 0.001 for week 32 vs week 40, P = 0.038 for week 32 vs week 41).

## 4. Discussion

The difficult and important step of fetal lung segmentation from ultrasound pictures is necessary for the computer-aided assessment of the fetal lung maturity. We proposed a novel automated technique for the segmentation of fetal lungs in ultrasound images. This research would help assess fetal development in terms of the physical characteristics of fetal organs as well as the quantitative analysis of fetal organs.

By training on 3500 annotated ultrasound images with 50 epochs, our proposed model demonstrated good performance in fetal lung segmentation with regard to accuracy, precision, recall, and IOU. Additionally, in validation dataset, theperformance of the Vgg16-GCN-UNet model was the best because its IOU and recall were higher than those of the competitors, as shown in Table 1. The generalization error plots of our model without cardiac and with cardiac have shown in Fig. 10 and Fig. 11. The Vgg16-GCN-UNet model outperformed the U-Net by 6.3% and 6.1% in IOU with and without cardiac annotations, respectively.In test dataset, the performance of the Vgg16-GCN-UNet model was also the best as shown in Table 2. The Vgg16-GCN-UNet model outperformed the U-Net by 9.8% and 7.3% in IOU testing with and without cardiac annotations, respectively.

We trained the Vgg16-GCN-UNet using the fetal lung ultrasound images with and without the cardiac annotation to examine the effects of the cardiac annotations on the segmentation of the fetal lungs. The contribution of cardiac area annotation to the lung segmentation can be shown by the comparison in Table 1 and Table 2. All the models that were trained using the data set with cardiac annotations outperformed

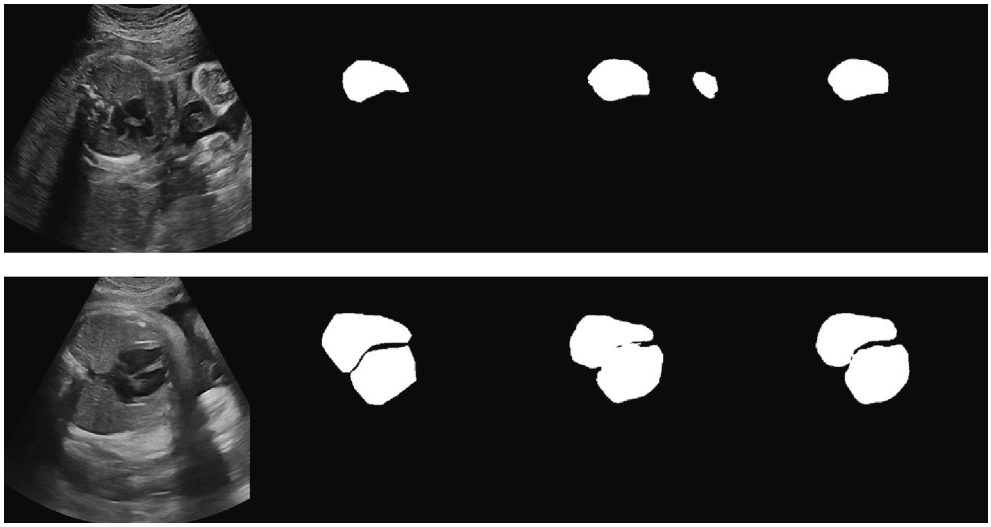

**Fig. 4.** Examples of fetal lung segmentation in Validation set.

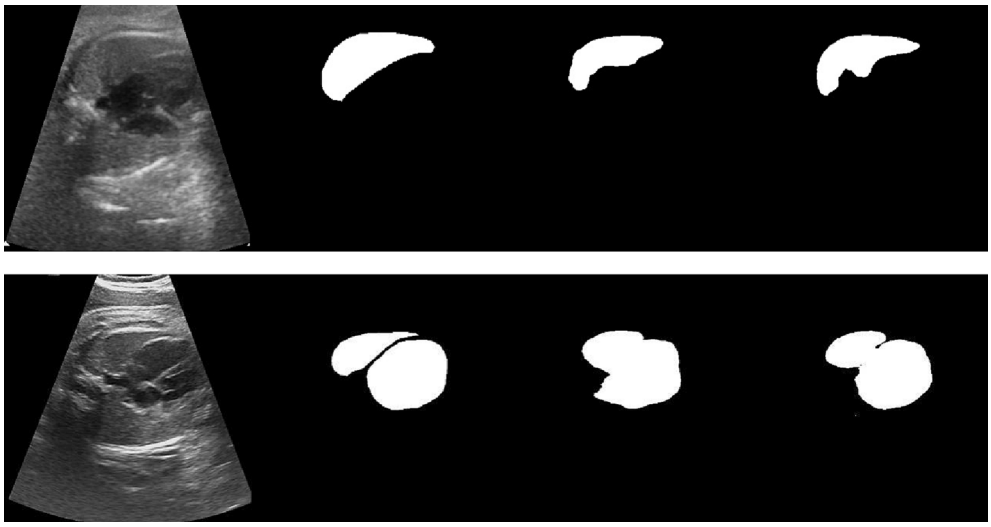

**Fig. 5.** Examples of fetal lung segmentation in Test set.

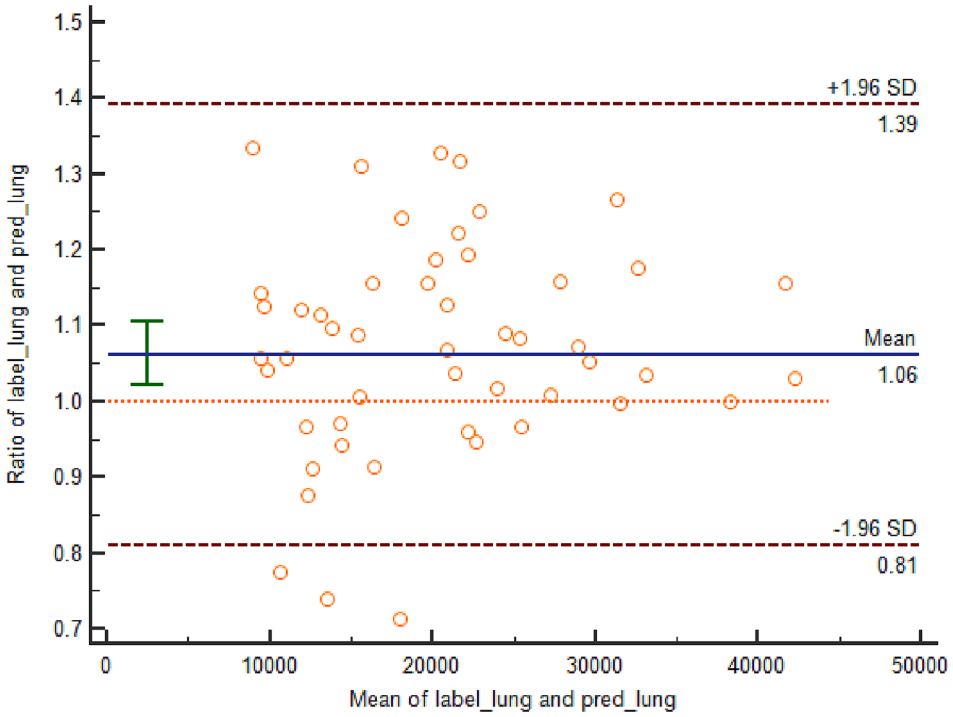


**Fig. 6.** Bland-Altman test for testing the agreement of fetal lung size between manual and auto segmentations.

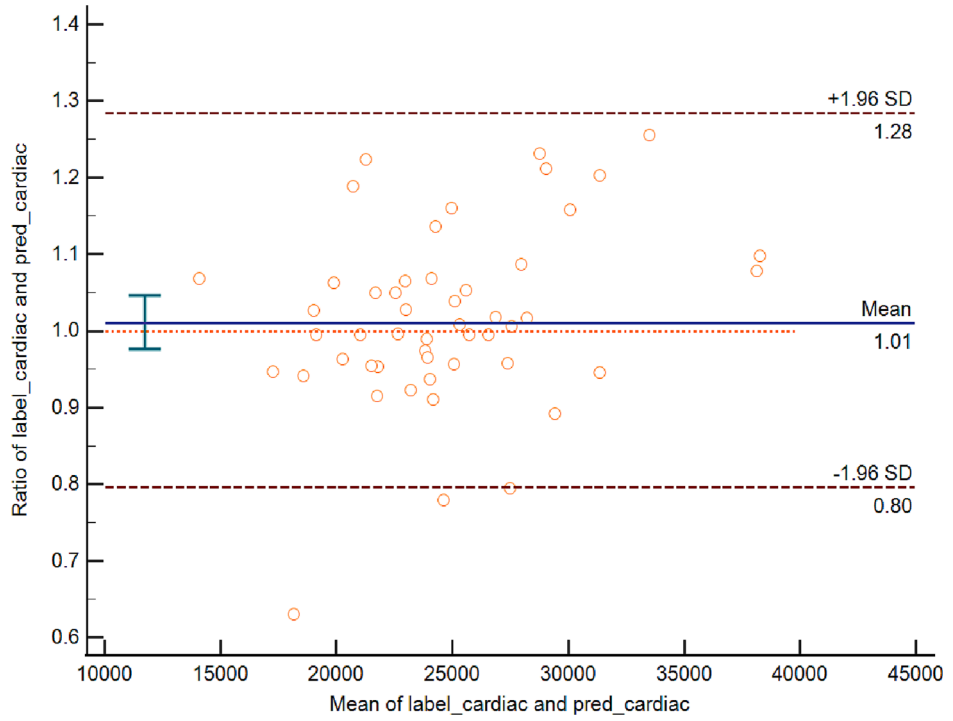


**Fig. 7.** Bland-Altman test for testing the agreement of fetal cardiac size between manual and auto segmentations.

their counterparts, as compared to the equivalents trained using the data set without cardiac annotations. These findings lead to the conviction that the lung annotations, when paired with cardiac region annotations, and Vgg16-GCN, both aided in the segmentation of the fetal lung. To execute the segmentation and interpret the data for the subsequent assessment of fetal development, our model Vgg16-GCN-UNet trained using fetal cardiac area annotations was deemed to be the best. In Fig. 4 and Fig. 5, the segmentation pictures of validation set and test set are displayed. In comparison to the actual data, the results demonstrate how correctly the suggested model can partition the lung area.

The recent similar works' performance in US has shown in Table 3. In recent similar studies, Li et. al. proposed a new method for semi-automatic segmentation of fetal lungs from fetal chest ultrasound images [42]. They applied the Expectation-Maximization (EM) algorithm to identify and obtain interesting frontiers. Their results presented were qualitative and no performance measures. They relied too much on the

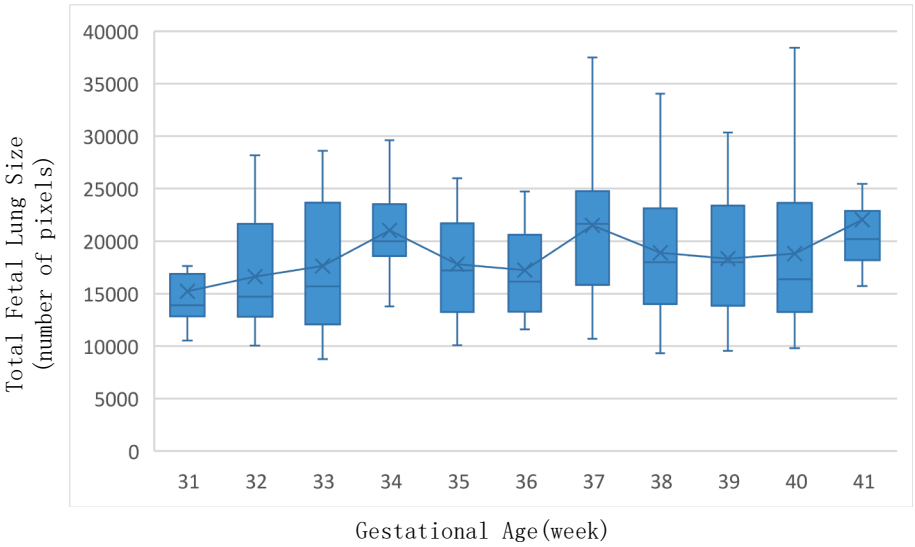


**Fig. 8.** Distribution of fetal lung size by gestational age. Box plot shows the variation of the fetal lung size by gestational age. X shape at each center of box denotes 50th percentile. Horizontal line inside the box represents mean value of fetal lung size. The top line and bottom line represent max and min value, respectively.

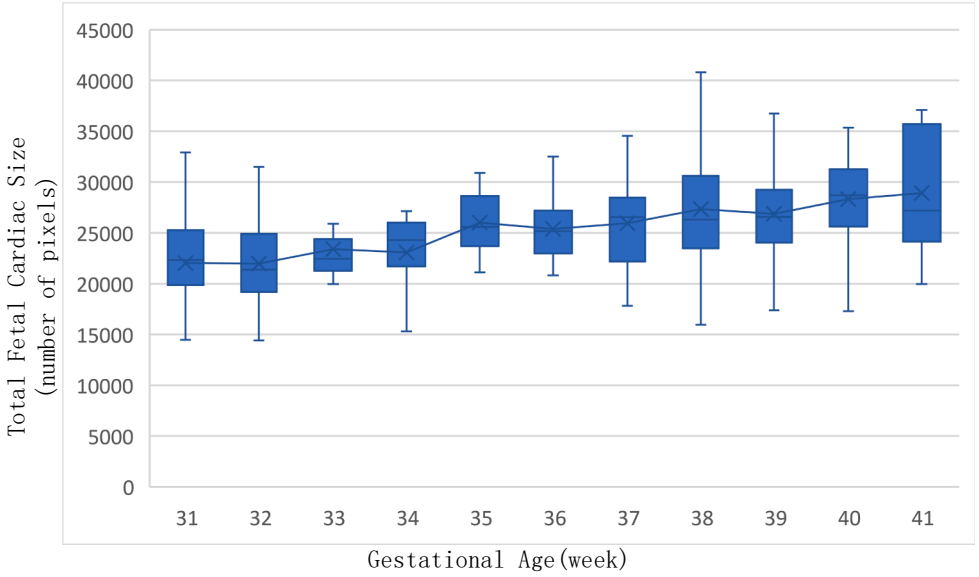


**Fig. 9.** Distribution of fetal cardiac size by gestational age.

final manual selection of experts, not the fully automatic segmentation algorithm we proposed. Xi et al proposed a model, which yielded a IoU of 77.0% for the segmentation of fetal lung [43]. Yin et al. proposed a U-net model to segment fetal lung with cardiac [44], which achieved a IoU of 79.0%. Our method achieved more IoU in the same task. Wang et al. provided a 2D segmentation of the fetal lungs in MRI, which coupled CNNs incorporated into a bounding box and a scribble-based pipeline [23]. The unsupervised DC is 0.85 ± 0.06 for the lungs. However, they used MRI which has no speckle noise and signal dropout of US to segment the fetal lung.

Healthy cardiorespiratory development is crucial to the life safety of the fetus. A multitude of pregnancy issues (e.g., Intrauterine Growth Restriction, Preeclampsia and Preterm Birth) may result in poor early heart development, eventually leading in fetal growth restriction or even death [45]. Fetal lung immaturity may produce Neonatal Respiratory Morbidity (NRM), described as neonatal respiratory distress syndrome or transitory shortness of breath, which may also lead to fetal morbidity or death [46]. Invasive evaluation procedures like amniocentesis may induce physical pain and a miscarriage risk of roughly 1.5% connected with the treatment [47]. Therefore, screening of prenatal cardiorespiratory problems utilizing non-invasive current medical imaging methods may be effective for assessing cardiorespiratory development and timely treatment of unwell fetus without disturbing the fetal development environment. Fetal lung segmentation would not only support computer-aided fetal lung assessment, such as texture analysis for predicting fetal lung maturity, but also help monitor fetal development.

Chen et. al. developed a deep learning model to evaluate fetal lung maturity using ultrasound images of four-cardiac-chamber view plane, with the hypothesis that the development of fetal lung maturity may be related to the texture information of the ultrasound images has been preliminarily proven [48]. However, the approach was challenged due to the difficulty in correctly determining gestational age. Nurmaini et. al. suggested a deep learning model for standard view segmentation of fetal cardiac echocardiogram, with well performed accuracy as 98.3% and 82.42% in intra-patient and inter-patient situations, respectively

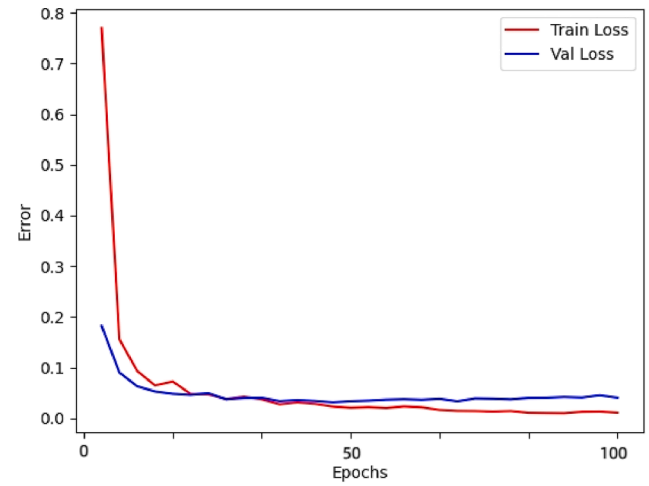


**Fig. 10.** The generalization error plots of our model without cardiac.

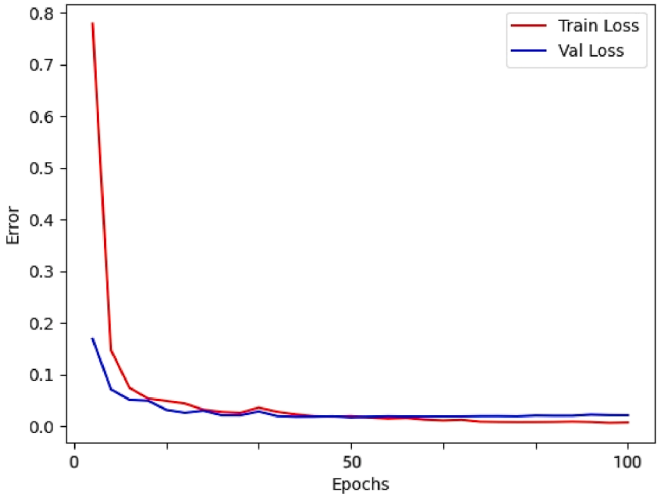


**Fig. 11.** The generalization error plots of our model with cardiac.

**Table 3**
Recent Similar Works' Performance in US.

| Method | Metric Accuracy | Recall | Precision | IOU |
|---|---|---|---|---|
| Li et. al without cardiac | qualitative | qualitative | qualitative | qualitative |
| Xi et al. without cardiac | 0.968 | 0.903 | 0.810 | 0.770 |
| Yin et al. with cardiac | 0.979 | 0.881 | 0.886 | 0.790 |
| **Our proposed modelwith cardiac** | **0.991** | **0.909** | **0.888** | **0.812** |

[49]. However, the research did not employ abnormal data such as VSDs, which may lead to biased outcomes. Dozen et. al. devised a unique U-net-based approach for segmenting the ventricular septum, termed crop-segment-calibration (CSC) [50]. Although the effectiveness of this approach is outstanding, it was cost-intensive and labor-intensive with its repeatability unproven.

In this study, we analyzed the fetal development in terms of the fetal lung/heart size at different gestational ages, taking advantages of the proposed model. Our results showed an increasing fetal lung size during 31st- 34th weeks and a subsequent decrease during 34th − 37th weeks and keep a steady state after 37th week which correlated with the previous publication [51]. Meanwhile, as showed in Fig. 9, the mean fetal cardiac area increased gradually with the development of the fetus from week 31 to week 41 ($P < 0.0005$), indicating that the fetal cardiac area may be potentially used to predict the gestational age. In clinics, the fetal heart size measurements can also be applied to predict the homozygosity for α-thalassemia-1 in mid-pregnancy effectively and non-invasively [52].

We proposed anovel automated model for segmenting the fetal lung in ultrasound images. The advantages included (1) Conventional CNN-based segmentation models Convolution neural network-based segmentation models only take care of local dependencies since convolutional kernel only sees visual information within the receptive field [53]. They ignore the full picture as a whole [54]. Our model could extract global features' relationship by GCN. (2) There is no fixed shape in human anatomies. The topological relationship extracted by GCN while performing representation learning has been proved stable against various application scenarios than that of the geometric relationship of general vision models, i.e., CNNs and ViTs [55]. In addition to the local features extracted by CNNs, GCN is also modeling the relationship among different local features. It optimizes local features of low-quality images by Laplacian smoothing to a certain extent [24], beneficial to promoting generation across data from different domains. (3) VGG16 could extract more abstract feature than normal CNN models, which has better respective field and performance.

However, the study had some limitations. First, GCN aggregates pixel blocks of the same category, but for small target segmentation with fewer pixels, the aggregation effect is not significant, and the improvement of semantic segmentation is limited. Second, the study's data analysis excluded the stage of rapid fetal lung development [5] and covered a limited range of gestational ages.Finally, our proposed model relies on a large set of manually annotated images for training that are expensive to acquire [56–58].

In future, we will introduce transformers architecture in our proposed model to model the small target in ultrasound images firstly. We will also collect data from multiple centers and multiple gestational weeks to increase the robustness of our proposed model and prepare for the actual landing deployment considering the above limitations.

## 5. Conclusions

In this paper, we proposed a novel U-shaped pre-trained architecture with a GCN bridge. It is capable of segmenting the fetal lung and heart across different scanners. Specifically, We employed a graph convolution network (GCN), a novel GCN-based bridge, to optimize the global space of intermediate feature layers. Empirical experiments on our dataset have demonstrated the effectiveness and robustness of the proposed architecture in fetal lung and heart segmentation. The limations of the work include (1) there were too many learnable parameters in this designed GCN bridge; (2) this study used single static ultrasound images as the input which may contain limited information. In the future, we may consider some easy Weisfeiler-Lehman algrithm to replace GCN model and video data as input. T.

**Institutional Review Board Statement:** The study was conducted in accordance with the Declaration of Helsinki, and approved by the Ethics Committee of Nanjing Medical University Affiliated Suzhou Hospital, Suzhou, China (Approval number: K2016038 and date of approval).

**Informed Consent Statement:** Informed consent was obtained from all subjects involved in the study.

**Data Availability Statement:** The data presented in this study are available on request from the corresponding author. The data are not publicly available due to privacy and ethical.

**Funding**

This research was funded by the National Natural Science Foundation of China (Grant No. 61975056), the Shanghai Natural Science Foundation (Grant No. 19ZR1416000), the Science and Technology Commission of Shanghai Municipality (Grant No. 20440713100, 19511120100), the National Natural Science Foundation of China (Grant No. 82151318), Scientific Development funds for Local Region

from the Chinese Government in 2023 (Grant No. XZ202301YD0032C), Jilin Province science and technology development plan project (Grant No. 20230204094YY). The authors would like to thank the reviewers in advance for their comments and suggestions.

## CRediT authorship contribution statement

**Jiangang Chen:** Conceptualization, Validation, Writing – review & editing, Project administration. **Size Hou:** Conceptualization, Methodology, Software, Validation, Formal analysis, Investigation, Writing – original draft, Writing – review & editing, Visualization. **Liang Feng:** Validation. **Bing Lu:** Data curation. **Minglei Yang:** Supervision. **Feiyang Sun:** Formal analysis. **Qingli Li:** Supervision. **Tao Tan:** Resources, Project administration. **Xuedong Deng:** Data curation. **Gaofeng Wei:** Supervision, Funding acquisition.

## Declaration of Competing Interest

The authors declare that they have no known competing financial interests or personal relationships that could have appeared to influence the work reported in this paper.

## Data availability

Data will be made available on request.

## Appendix A. Supplementary data

Supplementary data to this article can be found online at https://doi.org/10.1016/j.displa.2023.102451.

## References

[1] S. Robbiani, F. Tarantini, L. Ventura, C. Veneroni, L. Draghi, M.J. Dahl, J.J. Pillow, R.L. Dellacà, An implantable electronic device for monitoring fetal lung pressure in a lamb model of Congenital Diaphragmatic Hernia, IEEE Trans. Instrum. Meas. 18 (71) (2022 Jan) 1.
[2] M.J. Teune, S. Bakhuizen, C. Gyamfi Bannerman, et al., A systematic review of severe morbidity in infants born late preterm, Am. J. Obstet. Gynecol. 205 (4) (2011) 374.e371–374.e379.
[3] M. DeSilva, F.M. Munoz, M. Mcmillan, A. Tse-Kawai, H. Marshall, K.K. Macartney, J. Joshi, M. Oneko, A. Elliott-Rose, H. Dolk, F. Trotta, H. Spiegel, S. Tomczyk, A. Shrestha, S. Kochhar, E.O. Kharbanda, Congenital anomalies: case definition and guidelines for data collection, analysis, and presentation of immunization safety data, Vaccine 34 (49) (2016) 6015–6026.
[4] G. Kasprian, C. Balassy, P.C. Brugger, D. Prayer, MRI of normal and pathological fetal lung development, Eur. J. Radiol. 57 (2) (2006) 261–270.
[5] P. Vergani, M. Andreani, M. Greco, G. Farina, T. Fedeli, S. Cuttin, Two- or three-dimensional ultrasonography: which is the best predictor of pulmonary hypoplasia? Prenat. Diagn. 30 (9) (2010) 834–838.
[6] V.L. Ward, M. Nishino, H. Hatabu, et al., Fetal lung volume measurements: determination with MR imaging–effect of various factors, Radiology 240 (1) (2006) 187–193.
[7] D. Mahieu-Caputo, P. Sonigo, M. Dommergues, et al., Fetal lung volume measurement by magnetic resonance imaging in congenital diaphragmatic hernia, BJOG 108 (8) (2001) 863–868.
[8] M. Feingold, J. Scollins, C.L. Cetrulo, D. Koza, Fetal lung to liver reflectivity ratio and lung maturity, Journal of clinical ultrasound : JCU. 15 (6) (1987) 384–387.
[9] N. Mottet, C. Cochet, C. Vidal, et al., Feasibility of two-dimensional ultrasound shear wave elastography of human fetal lungs and liver: A pilot study, Diagn. Interv. Imaging 101 (2) (2020) 69–78.
[10] I. Tekesin, G. Anderer, L. Hellmeyer, W. Stein, M. Kühnert, S. Schmidt, Assessment of fetal lung development by quantitative ultrasonic tissue characterization: a methodical study, Prenat. Diagn. 24 (9) (2004) 671–676.
[11] M. Palacio, E. Bonet-Carne, T. Cobo, et al., Prediction of neonatal respiratory morbidity by quantitative ultrasound lung texture analysis: a multicenter study American Journal of Obstetrics and Gynecology. 217 (2) (2017), 196e191 196e114.
[12] D.G. Grenache, A.M. Gronowski, Fetal lung maturity, Clin. Biochem. 39 (1) (2006) 1–10.
[13] A.E. Besnard, S.A.M. Wirjosoekarto, K.A. Broeze, B.C. Opmeer, B.J. Mol, Lecithin/sphingomyelin ratio and lamellar body count for fetal lung maturity: a meta-analysis, European Journal of Obstetrics & Gynecology and Reproductive Biology. 169 (2) (2013) 177–183.
[14] J. Torrents-Barrena, G. Piella, NarcísMasoller, Eduard Gratacós, ElisendaEixarch, Mario Ceresa, Miguel Ángel González Ballester, Segmentation and classification in MRI and US fetal imaging: Recent trends and future prospects, Med. Image Anal. 51 (2019) 61–88.
[15] M.C. Fiorentino, F.P. Villani, M. Di Cosmo, E. Frontoni, S. Moccia, A review on deep-learning algorithms for fetal ultrasound-image analysis, Med. Image Anal. 14 (2022 Oct) 102629.
[16] S. Dahdouh, N. Andescavage, S. Yewale, A. Yarish, D. Lanham, D. Bulas, A.J. du Plessis, C. Limperopoulos In vivo placental MRI shape and textural features predict fetal growth restriction and postnatal outcome, J. Magn. Reson. Imaging 47 (2) (2018) 449–458.
[17] M. Havaei, A. Davy, D. Warde-Farley, et al., Brain tumor segmentation with Deep Neural Networks, Med. Image Anal. 35 (2017) 18–31.
[18] M.S. Hossain, Microcalcification Segmentation Using Modified U-net Segmentation Network from Mammogram Images, Journal of King Saud University - Computer and Information Sciences. (2019).
[19] Q. Hu, de F. Souza, LF, GB. Holanda, et al., An effective approach for CT lung segmentation using mask region-based convolutional neural networks, Artif. Intell. Med. 103 (2020) 101792.
[20] B. Kainz, D. Rueckert, Deepcut: object segmentation from bounding box annotations using convolutional neural networks, IEEE Trans. Med. Imaging 36 (2) (2017) 674–683.
[21] S. Chikop, S. Shiradon, P. Poojar, A. Arun, M.S. Muguru-Prabhuswamy, S. Pungavkar, S. Geethanath, Segmentation and visualization of brain and lung volumes in fetal MRI using active contours and morphological operators. Int. Society for Magnetic Resonance in Medicine (ISMRM) (2014) 6606.
[22] M. Rajchl, M. Lee, O. Oktay, K. Kamnitsas, J. Passerat-Palmbach, W. Bai, M. Rutherford, J. Hajnal, B. Kainz, D. Rueckert, Deepcut: object segmentation from bounding box annotations using convolutional neural networks, IEEE Trans. Med. Imaging 36 (2) (2017) 674–683.
[23] G. Wang, W. Li, M.A. Zuluaga, R. Pratt, P.A. Patel, M. Aertsen, T. Doel, A.L. David, J. Deprest, S. Ourselin, T. Vercauteren, Interactive medical image segmentation using deep learning with image-specific fine-tuning, IEEE Trans, Med Imaging, 2018.
[24] Han K, Wang Y, Guo J, et al. Vision GNN: An Image is Worth Graph of Nodes[J]. arXiv preprint arXiv:2206.00272, 2022.
[25] N. Dehmamy, A.-L. Barabási, Y.u. Rose, Understanding the representation power of graph neural networks in learning graph topology, Adv. Neural Inf. Proces. Syst. 32 (2019).
[26] Yang, Liang, et al. "Topology Optimization based Graph Convolutional Network." IJCAI. 2019.
[27] Jin, Di, et al., "Bite-gcn: A new GCN architecture via bidirectional convolution of topology and features on text-rich networks.", Proceedings of the 14th ACM International Conference on Web Search and Data Mining. (2021).
[28] T. Xiao, M. Singh, E. Mintun, et al., Early convolutions help transformers see better [J], Adv. Neural Inf. Proces. Syst. 34 (2021) 30392–30400.
[29] B.C. Russell, A. Torralba, K.P. Murphy, W.T. Freeman, LabelMe: A Database and Web-Based Tool for Image Annotation, Int. J. Comput. Vis. 77 (1) (2008) 157–173.
[30] M. Bloice, P.M. Roth, A. Holzinger, Biomedical image augmentation using Augmentor, Bioinformatics (Oxford, England). 35 (2019) 4522–4524.
[31] O. Ronneberger P. Fischer T. Brox U-Net: Convolutional Networks for Biomedical Image Segmentation 2015 Cham.
[32] Long J, Shelhamer E, Darrell T. Fully Convolutional Networks for Semantic Segmentation. arXiv e-prints. 2014:arXiv:1411.4038. https://ui.adsabs.harvard.edu/abs/2014arXiv1411.4038L. Accessed November 01, 2014.
[33] Q. Huang, Y. Huang, Y. Luo, F. Yuan, X. Li, Segmentation of breast ultrasound image with semantic classification of superpixels, Med. Image Anal. 61 (2020), 101657.
[34] Dahl GE, Sainath TN, Hinton GE. Improving deep neural networks for LVCSR using rectified linear units and dropout. Paper presented at: ICASSP, IEEE International Conference on Acoustics, Speech and Signal Processing - Proceedings2013.
[35] Ioffe S, Szegedy C. Batch normalization: accelerating deep network training by reducing internal covariate shift. Proceedings of the 32nd International Conference on International Conference on Machine Learning - Volume 37; 2015; Lille, France.
[36] G. Li, C. An, J. Yu, Q. Huang, Radiomics analysis of ultrasonic image predicts sensitive effects of microwave ablation in treatment of patient with benign breast tumors, Biomed. Signal Process. Control 76 (2022), 103722.
[37] K. Simonyan, A. Zisserman, Very Deep Convolutional Networks for Large-Scale Image Recognition, CoRR.2015, abs/1409.1556..
[38] Krizhevsky A, Sutskever I, Hinton GE. ImageNet classification with deep convolutional neural networks. Proceedings of the 25th International Conference on Neural Information Processing Systems - Volume 1; 2012; Lake Tahoe, Nevada.
[39] Q. Huang, H. Luo, C. Yang, J. Li, Q. Deng, P. Liu, M. Fu, L. Li, X. Li, Anatomical Prior Based Vertebra Modelling for Reappearance of Human Spines, Neurocomputing 500 (Aug 2022) 750–760.
[40] Yosinski J, Clune J, Bengio Y, Lipson H. How transferable are features in deep neural networks? Proceedings of the 27th International Conference on Neural Information Processing Systems - Volume 2; 2014; Montreal, Canada.
[41] Y Luo, Q Huang, X Li. Segmentation information with attention integration for classification of breast tumor in ultrasound image. Pattern Recognition 124, 108427.
[42] X. Li, Y. Wang, J. Yu, P. Chen. Fetal lung segmentation using texture-based boundary enhancement and active contour models. 3rd International Conference on Biomedical Engineering and Informatics (BMEI) (2010), pp. 264-268.
[43] J. Xi, J. Chen, Z. Wang, et al., Simultaneous Segmentation of Fetal Hearts and Lungs for Medical Ultrasound Images via an Efficient Multi-scale Model Integrated With Attention Mechanism, Ultrason. Imaging 43 (6) (2021) 308–319, https://doi.org/10.1177/01617346211042526.

[44] J. Yin, et al., Ultrasonographic segmentation of fetal lung with deep learning, Journal of Biosciences and Medicines 9 (1) (2021) 146–153.
[45] C.M.J. Tan, A.J. Lewandowski, The transitional heart: from early embryonic and fetal development to neonatal life[J], Fetal Diagn. Ther. 47 (5) (2020) 373–386.
[46] M. Palacio, T. Cobo, M. Martinez-Terron, et al., Performance of an automatic quantitative ultrasound analysis of the fetal lung to predict fetal lung maturity, Am. J. Obstet. Gynecol. 207 (6) (2012).
[47] M. Allyse, M.A. Minear, E. Berson, et al., Non-invasive prenatal testing: a review of international implementation and challenges[J], Int. J. Womens Health 7 (2015) 113.
[48] P. Chen, Y. Chen, Y. Deng, et al., A preliminary study to quantitatively evaluate the development of maturation degree for fetal lung based on transfer learning deep model from ultrasound images[J], Int. J. Comput. Assist. Radiol. Surg. 15 (8) (2020) 1407–1415.
[49] S. Nurmaini, M.N. Rachmatullah, A.I. Sapitri, et al., Deep learning-based computer-aided fetal echocardiography: application to heart standard view segmentation for congenital heart defects detection[J], Sensors 21 (23) (2021) 8007.
[50] A. Dozen, M. Komatsu, A. Sakai, et al., Image segmentation of the ventricular septum in fetal cardiac ultrasound videos based on deep learning using time-series information[J], Biomolecules 10 (11) (2020) 1526.
[51] M.L. Meyers, J.R. Garcia, K.L. Blough, W. Zhang, C.I. Cassady, A.R. Mehollin-Ray, Fetal Lung Volumes by MRI: Normal Weekly Values From 18 Through 38 Weeks' Gestation, Am. J. Roentgenol. 211 (2) (2018) 432–438.
[52] X. Li, X. Qiu, H. Huang, et al., Fetal heart size measurements as new predictors of homozygous α-thalassemia-1 in mid-pregnancy, Congenit. Heart Dis. 13 (2) (2018) 282–287.
[53] J. Torrents-Barrena, G. Piella, E. Gratacos, E. Eixarch, M. Ceresa, M.A. Ballester, Deep q-capsnet reinforcement learning framework for intrauterine cavity segmentation in TTTS fetal surgery planning, IEEE Trans. Med. Imaging 39 (10) (2020 Apr 14) 3113–3124.
[54] M. Raghu, T. Unterthiner, S. Kornblith, et al., Do vision transformers see like convolutional neural networks?[J], Adv. Neural Inf. Proces. Syst. 34 (2021) 12116–12128.
[55] G. Carlsson, R.B. Gabrielsson, Topological approaches to deep learning[M]// Topological data analysis, Springer, Cham, 2020, pp. 119–146.
[56] I. Wang, L. Guo D, G. Wang, S. Zhang, Annotation-efficient learning for medical image segmentation based on noisy pseudo labels and adversarial learning, IEEE Trans. Med. Imaging 40 (10) (2020 Dec 28) 2795–2807.
[57] Q. Huang, L. Ye, Multi-Task/Single-Task Joint Learning of Ultrasound BI-RADS Features, IEEE Trans. Ultrason. Ferroelectr. Freq. Control 69 (2) (2022) 691–701.
[58] Q. Huang, Z. Miao, S. Zhou, C. Chang and X. Li, "Dense Prediction and Local Fusion of Superpixels: A Framework for Breast Anatomy Segmentation in Ultrasound Image With Scarce Data," in *IEEE Transactions on Instrumentation and Measurement*, vol. 70, pp. 1-8, 2021, Art no. 5011508, doi: 10.1109/TIM.2021.3088421.